Thermal, moisture and mechanical properties of Seacrete

A sustainable sea-grown building material

Johra, Hicham; Margheritini, Lucia; Ivanov Antonov, Yovko; Meyer Frandsen, Kirstine; Enggrob Simonsen, Morten; Møldrup, Per; Lund Jensen, Rasmus

Published in:
Construction and Building Materials

DOI (link to publication from Publisher):
10.1016/j.conbuildmat.2020.121025

Publication date:
2021

Document Version
Accepted author manuscript, peer reviewed version

Construction and Building Materials

Thermal, Moisture and Mechanical Properties of Seacrete: A Sustainable Sea-Grown Building Material

Hicham Johra [a,*], Lucia Margheritini [a], Yovko Ivanov Antonov [a], Kirstine Meyer Frandsen [a], Morten Enggrob Simonsen [b], Per Møldrup [a], Rasmus Lund Jensen [a]

[a] *Aalborg University, Department of the Built Environment, Thomas Manns Vej 23, DK-9220 Aalborg Ø, Denmark.*
[b] *Aalborg University, Department of Chemistry and Bioscience, Niels Bohrs Vej 8, DK-6700 Esbjerg, Denmark.*

** Corresponding author. Tel.: +45 5382 8835. E-mail address: hj@build.aau.dk (H. Johra).*

Abstract

The ever-increasing global demand for concrete engenders concerning sustainability issues. In addition to the large CO_2 emissions induced by the production of cement, the fabrication of concrete requires important mining and excavation for the extraction of specific minerals, sand, and aggregates, which can endanger local ecosystems. Seacrete (also known as "Seament" or "Biorock") has previously been suggested as a potential alternative to traditional cementitious materials. Seacrete is artificial electrolytically precipitated calcium carbonate around a steel-frame cathode in which electrical current flows and that is submerged in seawater. Previous studies showed that it is ideal for the restoration of coral reefs and marine ecosystems. Furthermore, Seacrete is a very interesting sustainable concrete-like construction material for buildings and other human infrastructures. Indeed, it can be produced nearby all coastlines without any need for mining, extraction or transportation of additional material. In addition, the fabrication of Seacrete can easily be powered by low-intensity or local intermittent renewable energy sources. Previous publications pointed out that the mechanical properties and strength of Seacrete are similar to that of concrete, but no investigation has been conducted on other properties. For the first time, the current experimental study assesses the thermal and moisture properties of Seacrete. This article reports the density, compression strength, puncture resistance, specific heat capacity, thermal diffusivity, thermal conductivity, and water vapour sorption isotherms of two types of Seacrete, namely low-voltage and high-voltage Seacrete. Finally, this study emphasizes that all the aforementioned material properties of Seacrete are similar to that of concrete, confirming that the former can be considered for the construction of certain building elements and infrastructures.

Keywords: *Seacrete, Seament, Biorock, sustainable building material, material characterization, thermal properties, moisture properties, mechanical properties, hygroscopic properties, electrodeposition.*

Nomenclature

Latin symbols		
a_w	relative humidity in the VSA chamber	%
C	adsorption constants in the GAB model	-
C_p	Specific heat capacity	J/kg.K
K	adsorption constants in the GAB model	-
m	moisture content of the material at a dry state	% by mass
R^2	Coefficient of determination	-
W_m	monolayer capacity of the material	% by mass
Greek symbols		

α	Thermal diffusivity	m^2/s
θ	Temperature	°C
λ	Thermal conductivity	W/m.K
ρ	Density	kg/m^3
Acronyms		
DSC	Differential Scanning Calorimetry	
GAB	Guggenheim-Anderson-deBoer moisture transport model	
HV	High-Voltage	
LFA	Laser Flash Analysis	
LV	Low-Voltage	
RH	Relative Humidity	%
SEM	Scanning Electron Microscope	
SQX	Semi-Quantitative Analysis	
VSA	Vapour Sorption Analyzer	
XRD	X-Ray Diffraction	
XRF	X-Ray Fluorescence	

1. Introduction

Buildings account for nearly one-third of the worldwide final energy use and they are responsible for 39% of the global CO_2 emissions. Therefore, the building sector clearly appears as a key target to achieve the environmental and energy challenges of the 21st century, and mitigate the effects of global warming and climate change. A large part of the environmental footprint of the building sector actually lies in the energy, resources and CO_2 emissions embodied in the construction materials themselves. This is especially the case for buildings with a structure made of concrete [1]. This widely-used construction material presents very appreciable mechanical and thermal properties. However, its production has a large environmental impact. In order to supply the tremendous amount of concrete that is used by the construction sector, 830 000 000 tons of cement are produced each year [2], accounting for 5% - 8% of the global anthropogenic CO_2 emissions [3][4]. Moreover, the fabrication of concrete blocks requires important mining and excavation for the extraction of specific minerals, sand, and aggregates that are part of the composition of the former. Finally, a significant amount of freshwater is needed to prepare a concrete mix. As a consequence of the ever-increasing global demand for concrete [2], those natural resources are more and more scarce, which is at the root of certain emerging socio-political and economic tensions, and environmental problems. Sand and gravel are the most extracted materials in the world. The extensive extraction of the latter from rivers, beaches, and seafloors threatens the integrity of the local ecosystems but also undermines water and food security [5].

Among the potential alternatives to traditional cementitious materials, Seacrete has attracted some attention over the last years. Seacrete is artificial electrolytically precipitated calcium carbonate around a steel-frame cathode in which electrical current flows and that is submerged in seawater. The process of electro-accumulation of minerals dissolved in seawater to slowly grow rock-solid layers of limestone coatings around a steel-frame cathode was developed and patented by Wolf Hartmut Hilbertz in 1979 [6]. The naming “Seacrete” (also sometimes referred to as “Seament”) emphasizes the marine origin and the high mechanical resistance of this material (similar to concrete or cement). Indeed, previous studies have indicated that Seacrete material can present mechanical properties and strength that are similar to that of concrete [8]. Researchers indicated that the structural properties of Seacrete make it ideal for the restoration of coral reefs and marine ecosystems [8][9][10]. In the context of coral reefs restoration, the Seacrete material is commonly denominated as “Biorock” to emphasize its similarities with the organic coral skeleton. Seacrete is also a very interesting technology for on-site production of sustainable concrete-like construction material for buildings and other human infrastructures [9]. The four main advantages of Seacrete are as follows:

- It is literally produced out of the sea, in any desired shape or size, with no need of any excavation, mineral mining or transportation of additional materials (apart from the steel-frame cathode), which makes it a “fully-renewable” construction material (considering the vast reserves of calcium carbonate minerals dissolved in the oceans).
- It can be produced locally nearby all coastlines where 46% of the urban population and 39% of the entire world population lives [11].

- The production of Seacrete can easily be supplied by local low-intensity power sources (low voltage and low current) or intermittent renewable energy sources such as wind turbines, solar plants or wave energy converters.
- The production of Seacrete can be considered as a fully flexible electrical load for the electrical grid. The electrical demand (and associated yield) of the Seacrete production can be modulated to its full extent. This can be very beneficial for helping to balance electric grids with a high share of intermittent reviewable energy sources.

However, it should be noted that the current technology for Seacrete production has some limitations. The first estimates indicate that the energy needed for its fabrication is similar to that of cement: around 1000 kWh/kg [2][9]. However, it should be noted that there is a large variability in the mineral accretion rates for the electrodeposition technology, depending on many parameters of the marine environment such as temperature, salinity, pH, type of suspended particles, etc. [12]. In addition, contrary to what one could think and what some might claim, the formation of Seacrete by electrodeposition is not CO_2 neutral nor negative (it is not a carbon sink). Finally, the growth rate of the Seacrete layer around the cathode is restricted to only a few centimetres per year (depending on the applied voltage). This is an obvious limitation that does not allow the fast production of construction elements with Seacrete.

Previous publications about Seacrete only presented the mechanical characteristics of this material, but no investigation into its thermal and moisture properties has been carried out until now. The aim of this article is thus to provide, for the first time, the results and analysis of the thermal and moisture characterization tests performed on two different types of Seacrete: low-voltage (LV) and high-voltage (HV). In addition, three mechanical resistance tests have also been conducted. The different Seacrete characteristics are all compared to that of concrete (or cementitious mortar).

After the description of the Seacrete materials, their composition and production conditions, the different measurement methodologies for the determination of the mechanical, thermal and moisture properties are presented. The results of these experimental tests are then analysed to obtain the (dry bulk) density, compression strength, puncture resistance, specific heat capacity, thermal diffusivity, thermal conductivity, and water vapour sorption isotherms of the two types of Seacrete. The article closes with a summary of all the main results of this experimental study, followed by conclusions and suggestions for future work on this topic.

2. Materials

This experimental study analyzes two different types of Seacrete material: an LV Seacrete, and an HV Seacrete. As indicated by their names, they were produced at different growth-rates by electro-accumulation around a cathode subjected to different voltages (potential differences), and in which electrical current flows at different intensities. For comparison, the same experimental analyses for mechanical and hygric properties are also conducted on a sample of cementitious mortar. For the sake of simplicity, this cementitious mortar is referred to as “concrete” in the rest of the article, even though it is not a concrete sensu stricto. Regarding the comparison of thermal properties, values found in scientific literature and international standards for calcium carbonate minerals, Brucite minerals and concrete are used. The description, composition, and production method of the tested materials are detailed hereafter.

2.1. Material production

Induced mineral deposition in seawater is achieved through electrolysis. This process only requires a simple system of two electrodes: an anode and a cathode. When an electrical potential difference is applied, the anode becomes positively charged and the cathode becomes negatively charged. This induces the precipitation of some of the elements dissolved in seawater (i.e. Mg^{2+}, Ca^{2+}) on the cathode. The deposition of calcium carbonate ($CaCO_3$) is common in the field of cathodic protection of steel and reinforced concrete elements and has therefore been widely investigated [13].

The low-voltage Seacrete material of this study originates from a Seacrete production installation located in Thailand, in which a very low voltage of 2.5 V is applied [14]. The high-voltage Seacrete material has been formed around the Italy-Greece submarine power cable by parasitic currents appearing on the latter after its protection sheath had disappeared. The maximum tension in this power cable is estimated to be around 400 000 V. These conditions enhanced the precipitation of Mg^{2+}, which resulted in the formation of an HV Seacrete that is softer and presents a higher porosity than the LV Seacrete [7].

Table 1: *Origin and production conditions of the low-voltage [14] and high-voltage Seacrete materials [7].*

Material	Low-voltage Seacrete	High-voltage Seacrete
Origin	Ko Tao Island - Thailand	Otranto – Italy
Water temperature	25 °C – 31 °C	3 °C – 24 °C
Water depth	12 m	35 m
Voltage	~ 2.5 V	400 000 V
Estimated time of formation	3 months	12 months
Growth rate (around cathode)	0.8 cm / year	5.5 cm / year

The difference in the formation of LV and HV Seacrete lies in the variation of pH nearby the cathode. The reduction of seawater in the proximity to the cathode generates a local increase of the pH close to it. This higher pH thus results in $CaCO_3$ precipitating at the surface of the electrode. Under standard seawater conditions, calcium carbonate can form two different crystal forms: Aragonite and Calcite. Previous experiments have shown that increasing the current in the electrodes above a certain level results in the electrodeposition of magnesium hydroxide ($Mg(OH)_2$, Brucite) rather than $CaCO_3$. Brucite is a softer (lower mechanical resistance) mineral than Aragonite and Calcite [9]. The precipitation of Brucite occurs when the pH at the surface of the electrode reaches 9.2 [15].

Regarding the CO_2 budget of the calcium carbonate precipitation, one could intuitively think that since limestone deposition is removing dissolved inorganic carbon from the ocean, this should be compensated by absorption of atmospheric CO_2 into the ocean. However, the opposite phenomenon occurs. This can be explained by the fact that there is actually much more dissolved inorganic carbon in the ocean (in the form of bicarbonate ion HCO_3^-) than there is CO_2 in the atmosphere. Consequently, the predominant reaction for the precipitation o calcium carbonate is as follows:

$$Ca^{++} + 2HCO_3^- = CaCO_3 + H_2O + CO_2$$

Therefore, for every two molecules of bicarbonate precipitated as limestone in the ocean, one molecule of CO_2 is released into the atmosphere. On the geological time scale, this is the major source of atmospheric CO_2 along with volcanic activity [9]. More information about Seacrete and materials formed by electrodeposition of minerals in seawater can be found in the publications of Goreau [9][10].

The concrete sample used for the comparison tests is a standard normal-weight 25 MPa (compression strength class C20/25 [16]) cementitious mortar composed of white Portland cement (Aalborg White® type CEM I 52.5 R [17]) and sand 0-4. It was produced with a water-cement mass ratio of 0.7 and a sand-cement mass ratio of 4. The mechanical resistance of this cementitious mortar is not very high, but it is suitable for low-rise indoor constructions.

2.2. Material description and composition

One can see in *Figure 1* the images and the scanning electron microscope (SEM) images of the tested LV Seacrete, HV Seacrete and cementitious mortar/concrete.

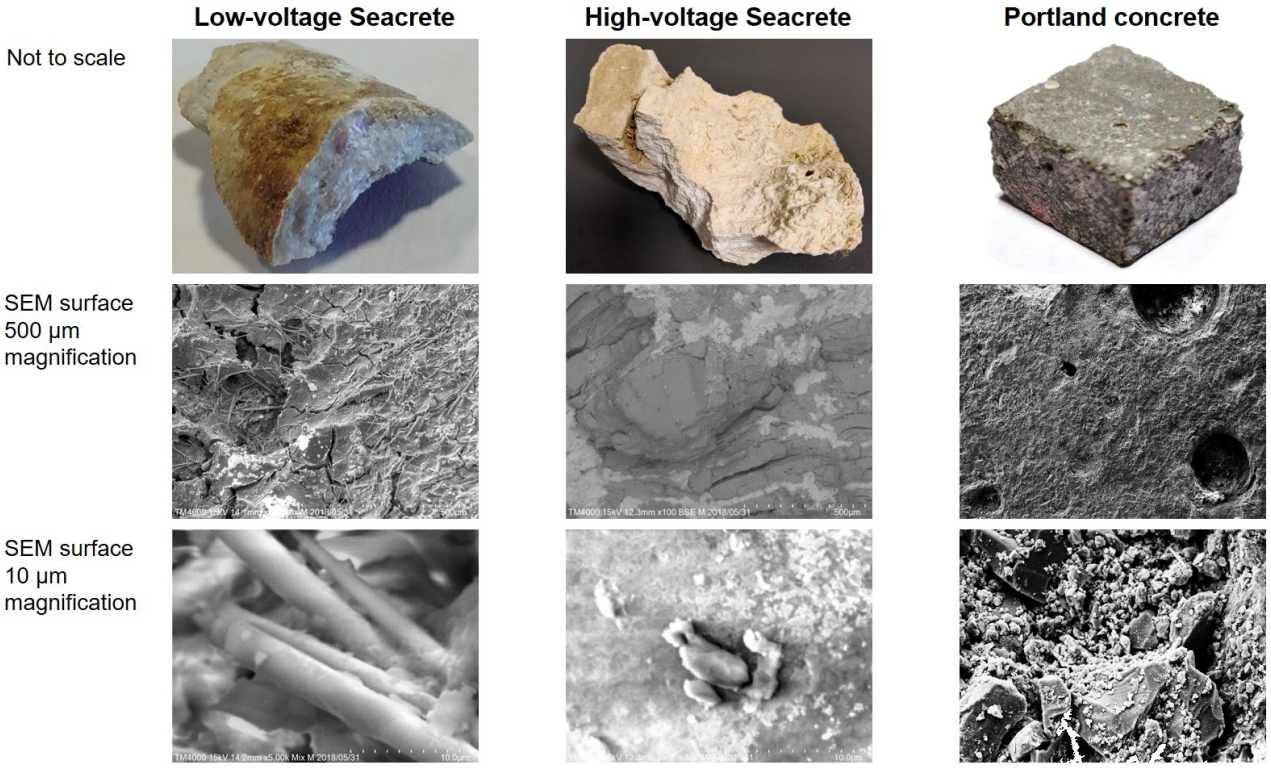

Figure 1: *Pictures of the tested materials: low-voltage Seacrete, high-voltage Seacrete, cementitious mortar/concrete (top); scanning electron microscope images of the surface of the tested materials (centre end bottom) [7].*

One can see in *Table 2* that the LV Seacrete is composed of 80.8% Aragonite, 18.9% Brucite, and 0.3% Calcite. The HV Seacrete is composed of 46.6% Aragonite, 52.3% Brucite, and 1.1% Calcite. As previously mentioned, Aragonite and Calcite are some of the mineral forms of calcium carbonate $CaCO_3$. Brucite is the mineral form of magnesium hydroxide $Mg(OH)_2$. The details of the chemical composition of the Seacrete test samples can be found in *Table 3*.

Table 2: *Quantitative composition analysis on X-ray Diffraction (XRD) tests for the low-voltage and high-voltage Seacrete materials [7].*

Mineral	**Low-voltage Seacrete mass content [mass%]**	**High-voltage Seacrete mass content [mass%]**
Aragonite	80.8	46.6
Brucite	18.9	52.3
Calcite	0.3	1.1

Table 3: *Semi-Quantitative Analysis (SQX) on X-ray Fluorescence (XRF) tests for the low-voltage and high-voltage Seacrete materials [7].*

No.	**Element**	**Low-voltage Seacrete mass content [mass%]**	**High-voltage Seacrete mass content [mass%]**
1	Mg	26.8	49.2
2	Al	0.385	0.754
3	Si	2.15	2.68
4	P	0.155	0
5	S	0.528	0.292
6	Cl	1.01	0.273
7	K	0.263	0.269
8	Ca	66.2	45
9	Fe	0.952	0.378

10	Ge	0.114	0
11	As	0.125	0.11
12	Sr	1.34	1.02

3. Measurement methods

This section describes the different experimental methods used to determine the density, compression strength, puncture resistance, specific heat capacity, thermal diffusivity, thermal conductivity, and water vapour sorption isotherms of the test samples. Information about the preliminary conditioning of the tested samples is also provided. Apart from the penetration test used to determine the puncture resistance, all other material properties have been assessed with standard characterization methodologies on state-of-the-art measurement equipment.

3.1. Measurement of the density

The density (dry bulk density of the material including voids) of the tested sample is measured with the well-known and commonly used Archimedes' principle of buoyancy [18] on a precision scale. The immersion fluid used for the density measurement is ethanol. Both the ethanol and the test sample are stabilised at room temperature of 20 °C before and during the measurement. Ten consecutive mass measurements are performed to calculate the mean average density of the tested sample. The measurement uncertainty is assessed with the standard deviation (1σ for a confidence region of 68.3%) of these consecutive measurements.

3.2. Measurement of the mechanical resistance

Due to of the limited amount of Seacrete material available for this study, it was not possible to prepare 4 x 4 x 4 cm cubical samples for standard compression strength tests according to the standard BS EN 196-1:2016 [19]. The largest available cubical samples of HV Seacrete are 1 x 1 x 1 cm in dimensions. The largest available samples of LV Seacrete are ~1 x 1 x 0.4 cm in dimensions (non-uniform shape).

A scaled-down version of the compression strength test for 4 x 4 x 4 cm cubical sample is thus conducted on 1 x 1 x 1 cm HV Seacrete samples. For the LV Seacrete, a non-standard penetration test is performed to measure puncture resistance. The non-standard penetration test is also carried out on the HV Seacrete samples. To verify that the results of the scaled-down compression and the penetration tests are comparable to a standard compression test on a 4 x 4 x 4 cm cubical sample, the cementitious mortar/concrete material is also tested with all three aforementioned tests.

3.2.1. Measurement of the compression strength

Compression testing is performed using a state-of-the-art automated material testing system MTS 810 from MTS Systems Corporation [20]. The experimental protocol follows the method described in the standard BS EN 196-1:2016 [19], except for the sample dimensions. Compression strength was determined for three samples of dimensions 1 x 1 x 1 cm for both HV Seacrete and concrete. The compressive strength is determined using standard stress/strain relation.

3.2.2. Measurement of the puncture resistance

The experimental setup for determining the puncture resistance is shown in *Figure 2*. It consists of a cylindrical puncture tip mounted on a controlled hydraulic piston applying force at a constant rate onto the test sample. The apparatus records the applied force as a function of displacement. The tested samples are embedded in high strength concrete matrix to ensure proper support and prevent any movement of the samples during the experiment. The composition and strength of this concrete matrix are the same for all tested samples. The size and shape of the LV Seacrete sample were adequate for only one penetration test. Concerning the HV Seacrete and concrete materials, two samples with dimensions 1 x 1 x 1 cm were tested using the same setup. The mechanical puncture resistance is assessed as the maximum applied force before rupture of the sample's surface. It should be noted that this puncture resistance test is non-standard but similar to the standard micro- or nano-indentation tests that are commonly conducted to assess the hardness of such materials. However, for this non-standard puncture resistance test, the displacement of the puncture tip is significantly larger than that of a micro-indentation test. In that situation, the properties of the concrete support matrix can influence the test results. Therefore, the latter should only be considered as a relative comparison between the tested samples.

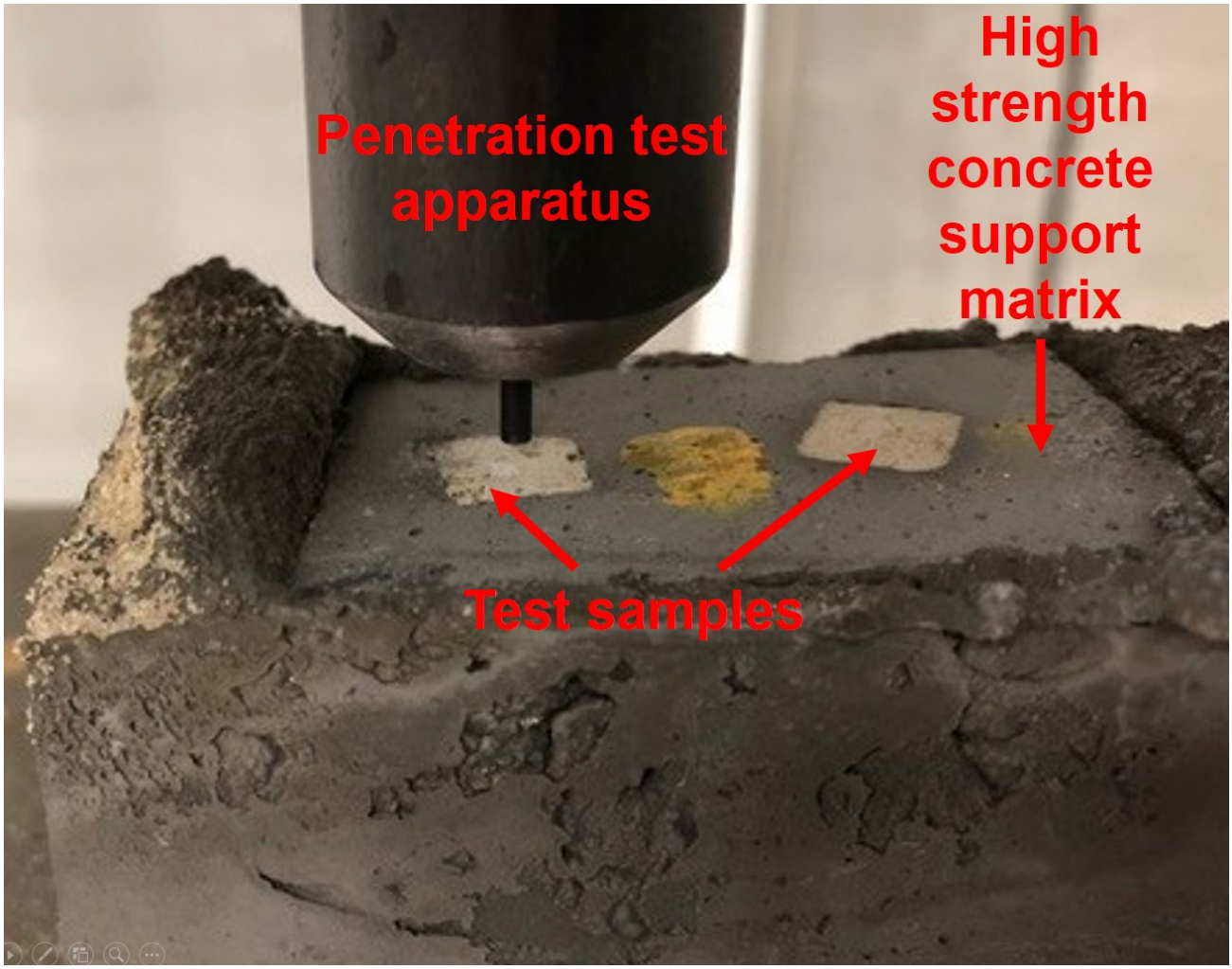

Figure 2: *View of the penetration test performed on the low-voltage Seacrete, the high-voltage Seacrete and the concrete samples to measure their puncture resistance.*

3.3. Measurement of the thermal properties

In this section, the methodology used to assess the thermal properties of the Seacrete samples is presented. The specific heat capacity and the thermal diffusivity of the material are directly measured with state-of-the-art experimental methodologies and laboratory equipment. Once known, the latter can be used together with the density measurement results to calculate the thermal conductivity of the material. The measurement uncertainty of the specific heat capacity and the thermal diffusivity is assessed with the standard deviation (1σ for a confidence region of 68.3%) of these respective measurements at a given temperature. The uncertainty of the calculated thermal conductivity is obtained with a simplified error propagation assuming independent variables and no covariance terms [21].

3.3.1. Measurement of the specific heat capacity

The specific heat capacity of the Seacrete samples is measured with the Differential Scanning Calorimetry (DSC) method [22]. It consists of the precise measurement of heat required to increase the temperature of the test sample as a function of the temperature of the latter. In the current investigation, the specific heat capacity measurements are performed at temperatures ranging from -60°C to 90°C with a DSC Q2000 apparatus from TA Instruments, Inc. [23]. The tested samples placed in the DSC apparatus are smaller fragments cut from the original Seacrete samples. These fragments have been polished to produce a flat and even surface to ensure good thermal contact between the sample and the DSC crucible, in order to avoid thermal gradient inside the sample and thus obtain reliable results.

3.3.2. Measurement of the thermal diffusivity

The thermal diffusivity of the Seacrete samples is measured with the Laser Flash Analysis (LFA) method [24]. It consists in illuminating one side of the test sample with a high-intensity and short-duration laser flash pulse, and measure the change of temperature over time on the other side with an infrared detector. The transient temperature response of the Laser Flash experiment can then be fitted by a mathematical model. The latter outputs the thermal diffusivity of the tested sample. In the current investigation, the thermal diffusivity measurements are performed at temperatures ranging from 10°C to 60°C with an LFA 447 apparatus from Netzsch Gerätebau GmbH [25]. The tested samples placed in the LFA apparatus are smaller fragments cut from the original Seacrete samples. This fragment has been polished in order to get disk-shaped samples with a diameter of 9.82 mm and 23.54 mm for the LV and the HV Seacrete samples, respectively. It should be noted that the size of the LV Seacrete sample is smaller than that of the HV Seacrete because of the limited size of the original LV Seacrete sample. The test samples have regular and even flat surfaces, with a thickness of 2.774 mm and 3.376 mm, and a mass of 0.4033 g and 2.6021 g for the LV and HV Seacrete samples, respectively. In addition, the Seacrete samples are coated with high absorption graphite spray in order to ensure a good and homogenous laser absorption on the illuminated face of the samples, and a good temperature measurement on the other face by the infrared detector. During the data analysis, the model used to fit the Laser Flash experiment and extract the material thermal diffusivity is the "radiation + pulse correction" model. The latter is the most appropriate for this type of material.

3.3.3. Calculation of the thermal conductivity

Based on the density measurements at ambient temperature (20°C), the thermal diffusivity measurements, and the specific heat capacity measurements of the Seacrete samples, the thermal conductivity of the latter within the temperature range 10 – 60°C is calculated with the following equation:

$$\boldsymbol{\lambda(\theta) = \rho(20°C) \times \alpha(\theta) \times C_p(\theta)} \quad (1)$$

Where λ, ρ, α, C_p and θ are the thermal conductivity [W/m.K], density [kg/m^3] (here measured at a constant temperature of 20 °C), thermal diffusivity [m^2/s], specific heat capacity [J/kg.K], and temperature [°C], respectively.

3.4. Moisture sorption-desorption capacity

In this study, the moisture properties of the tested materials are characterized by the measured sorption-desorption isotherms, hysteresis and the surface area of the material. A water vapour sorption isotherm is the curve describing the relationship between the water content in a material and the relative humidity of its surrounding environment at a given constant temperature. The difference between the adsorption curve (when the relative humidity is increasing) and the desorption curve (when the relative humidity is decreasing) at a given relative humidity is designated as hysteresis.

Water vapour sorption isotherms are determined for all three materials, using the commercially available Vapour Sorption Analyzer (VSA) from Aqualab [26]. This instrument can measure the sorption and desorption isotherms automatically using one of the two available state-of-the-art methods. The experimental method applied for this study is the "Dynamic Dew-point Isotherm". In the latter, a small sample placed in the VSA chamber is automatically wetted and dried using the chilled mirror dew-point technique. A high-precision mass scale continuously monitors the mass of the sample. The measurement is conducted for a relative humidity ranging from 3% to 93% with a step increment of approximately 4%, at a constant temperature of 23 ºC. With the VSA apparatus, an isotherm is determined in approximately 24 hours. This is a much faster testing time than standard methods for determination of isotherms (defined in EN 12571:2013 [27]). It is thus possible to run several consecutive tests on the same sample, which has be shown to be very useful for obtaining time-dependent moisture behaviour of material throughout sorption-desorption cycles [28]. To investigate the repeatability moisture dynamics from one cycle to the next, each material sample is consecutively tested twice with identical boundary conditions, without removing the sample from the VSA chamber.

The measured sorption-desorption isotherm data is then used to calculate the coefficients of the well-known moisture transport model Guggenheim-Anderson-deBoer (GAB). The GAB model is described by the following equation:

$$\boldsymbol{m = \frac{W_m K C a_w}{(1 - K a_w)(1 - K a_w + K C a_w)}} \quad (2)$$

Where m is the moisture content of the material [kg water/kg dry mass or % by mass], a_w is the water activity or relative humidity [%] in the surrounding environment, W_m is a parameter representing the monolayer capacity of the material [kg water/kg dry mass or % by mass], C is a dimensionless adsorption constant representing the difference in free enthalpy in the pure liquid state and the monolayer, and K is a dimensionless adsorption constant representing the difference in free enthalpy of water molecules in pure liquid state and in the layers above the monolayer [29][30]. The amplitude of the sorption-desorption hysteresis is calculated as the difference of moisture content between the adsorption and the desorption curves at 25% RH, 50% RH and 75% RH. From the isotherm measurements, the surface area of the material [m^2/gr] can be approximated by a method that is commonly used for soil characterization [31]. Assuming that a monolayer of water molecules (a layer with thickness of one single molecule) is present at 21% RH, the material water active surface area can be estimated with the following equation:

$$surface\ area = \frac{water\ content}{18.0152} * (10.8 * 10^{-20} * 6.022045 * 10^{23}) \quad (3)$$

4. Results and discussion

4.1. Density measurements

The measured density of the LV Seacrete sample is 2499.2 kg/m³ (with a 1σ standard deviation of 9.1 kg/m³). This density is comparable to that of the three common forms of calcium carbonate: Aragonite with a density of 2950 kg/m³ [32][33], Vaterite with a density of 2540 kg/m³ [32][34], and Calcite with a density of 2710 kg/m³ [32][35]. This result is logical since the LV Seacrete material is mostly composed of Aragonite mineral. The second main mineral composing the LV Seacrete is Brucite ($Mg(OH)_2$), which has a density of 2390 kg/m³ [36]. The measured density of the HV Seacrete sample is 1771.1 kg/m³ (with a 1σ standard deviation of 17.4 kg/m³). This density is significantly lower than that of the LV Seacrete, the three common forms of calcium carbonate, and Brucite (the main component of the HV Seacrete). This result can be explained by the higher porosity of the HV Seacrete compared to the LV Seacrete. Nonetheless, a previous study showed that the solid density (density of the pure solid phases excluding voids) of the HV Seacrete is close (although slightly smaller) to the one of the LV Seacrete: 2240 – 2540 kg/m³ and 2700 kg/m³, respectively [7]. Finally, the concrete sample used for comparison tests has a density of 2122.4 kg/m³, which is considered normal-weight class concrete [16].

One can see in *Figure 3* the comparison between the density of the Seacrete samples and other common building and construction materials. It is noticeable that the LV Seacrete, like the other forms of calcium carbonate, has a similar density to normal-weight and heavy-weight concretes or dense natural stones that are commonly used as construction material for structural elements in buildings. Regarding the HV Seacrete, its density is comparable to that of the high range of the light-weight concretes or medium-density natural stones [16][37].

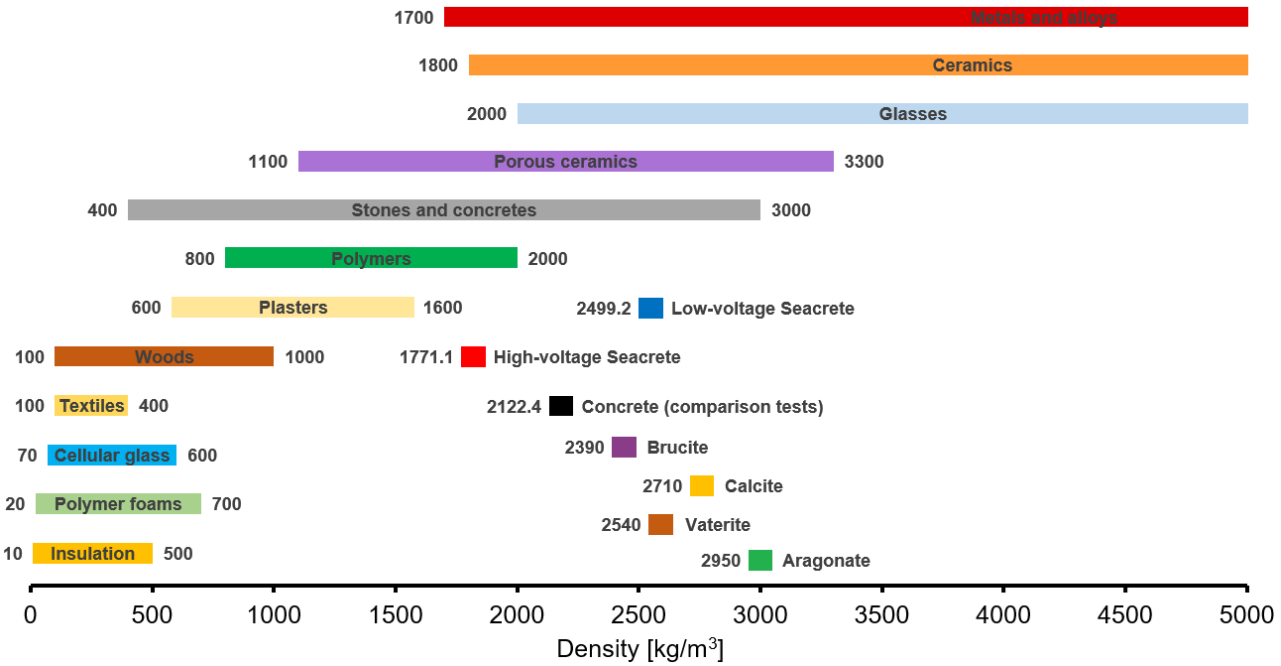

Figure 3: *Density comparison of the low-voltage Seacrete and the high-voltage Seacrete with other common building and construction materials [37].*

4.2. Mechanical resistance measurements

The results of the different mechanical resistance tests are summarized in *Table 4.* The compression strength for concrete and HV Seacrete are obtained using the standard stress-strain relation (average of three tests). The compression strength of the concrete sample is 25.1 MPa for the standard test on a 4 x 4 x 4 cm cubical sample, corresponding to a compressive strength class C20/25 [16], which is common for low-rise indoor constructions. One can observe that the results for 1 x 1 x 1 cm and 4 x 4 x 4 cm cubical concrete samples are very similar. It can thus be concluded that results from the scaled down compression tests are comparable to the standardized compression test on a 4 x 4 x 4 cm cubical sample. The compression resistance of the HV Seacrete is significantly lower than that of the concrete. This can be explained by the fact that HV Seacrete is mostly composed of Brucite, a mineral that is softer than Aragonite and Calcite which compose most of the LV Seacrete. In addition, HV Seacrete presents a higher porosity with more open pores, and therefore a weaker resistance in its mineral matrix. Nevertheless, it is within the range of compression strength class C12/15, which is the minimum compression strength for applications if there is no risk of corrosion or attack [16].

Table 4: *Mechanical resistance measurements for the low-voltage Seacrete, the high-voltage Seacrete and the concrete.*

Mechanical test	Mechanical property	Low-voltage Seacrete	High-voltage Seacrete	Concrete
Compression test on 4 x 4 x 4 cm cubical sample (standard)	Compression strength	Not measured	Not measured	25.1 MPa
Compression test on 1 x 1 x 1 cm cubical sample (down scaled)	Compression strength	Not measured	16.8	24.2 MPa
Penetration test on 1 x 1 x 0.4 cm or 1 x 1 x 1 cm cubical sample (non-standard)	Puncture resistance	3.9 kN	1.4 kN	3.4 kN

Figure 4 shows the results of the penetration test illustrated in *Figure 2*. These results are presented in the form of displacement as a function of applied force. The puncture resistance is thus determined as the maximum applied force onto the sample before the first break (rupture of the sample's surface). One can observe in *Figure 4 s*uccessive drops in the applied force. This is due to the successive ruptures of the different material layers in the sample.

From *Table 4* and *Figure 4*, it may be observed that the LV Seacrete presents a puncture resistance that is very close to that of the tested concrete. This can be explained by the relatively low porosity of the LV Seacrete and the fact that the Calcite and Aragonite composing the former are relatively hard minerals. Therefore, one could reasonably extrapolate that the LV Seacrete has a similar compression strength as the tested concrete, and thus has a compressive strength of class C20/25. Similarly to the compression resistance test, the HV Seacrete has a significantly lower puncture resistance when compared to LV Seacrete and concrete. As mentioned above, this is due to its higher porosity and the relative softness of the Brucite mineral.

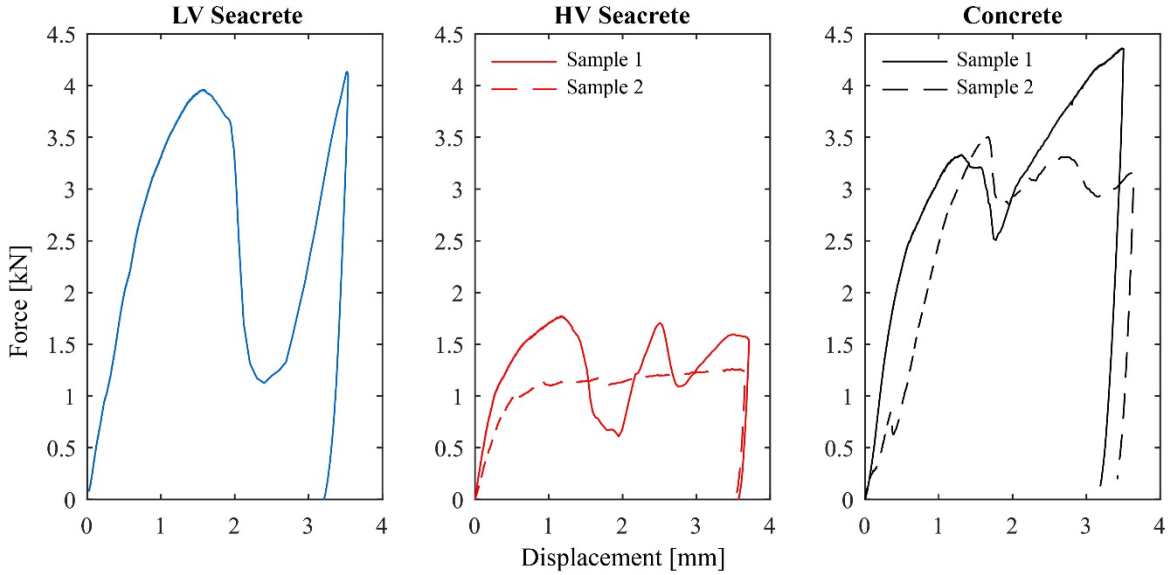

Figure 4: *Measurement data from the penetration test on the low-voltage Seacrete, the high-voltage Seacrete and the concrete samples (1 x 1 x 0.4 cm or 1 x 1 x 1 cm cubical sample embedded in concrete matrix).*

4.3. Thermal properties measurements

4.3.1. Specific heat capacity measurements

One can see in *Figure 5* and in *Table 5* the specific heat capacity measurements of the Seacrete samples within the temperature range -60 °C to 90 °C. It can be noted that the measured specific heat capacities of the LV Seacrete and the HV Seacrete are very close to each other. One can also observe that, within that temperature range, the specific heat capacity of Seacrete tends to increase linearly with the increasing temperature.

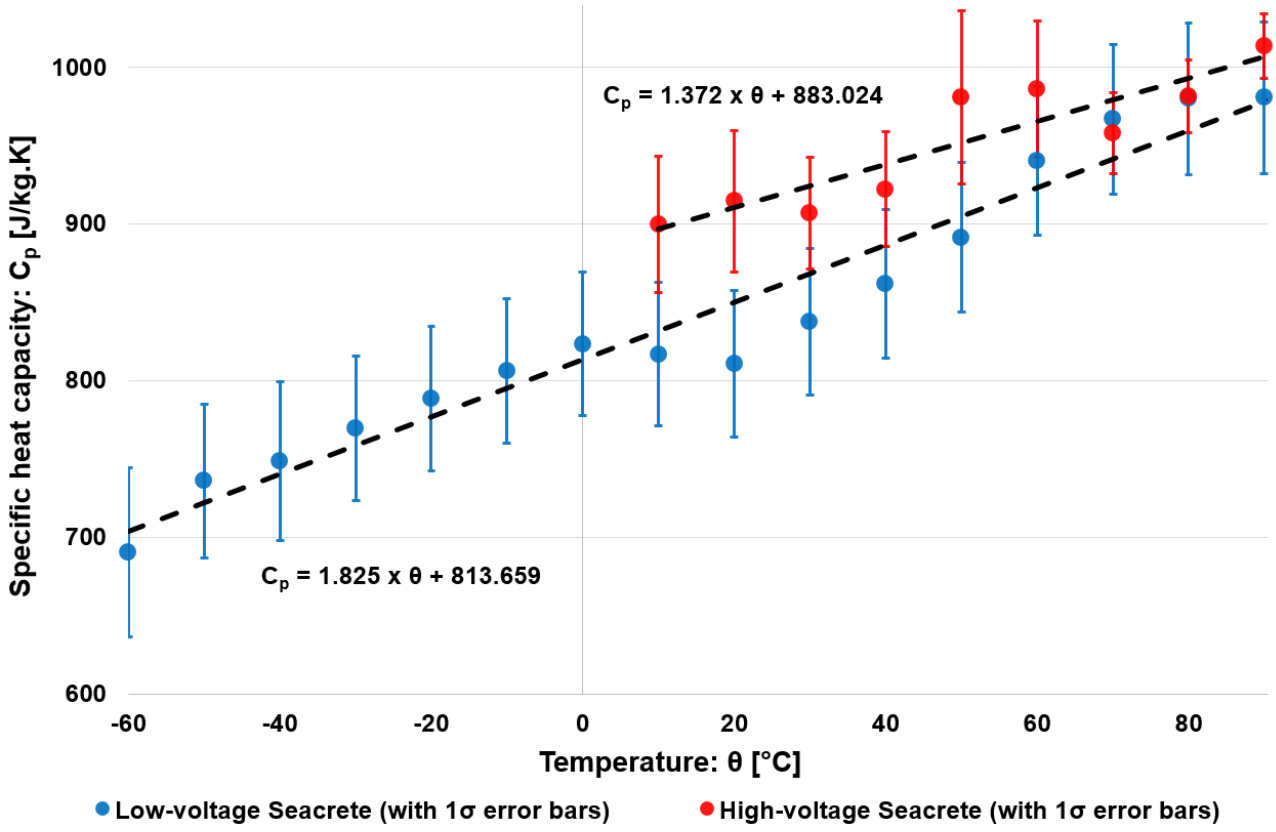

Figure 5: *Measurements of the specific heat capacity of the low-voltage Seacrete and the high-voltage Seacrete as a function of temperature with linear fitting functions.*

Table 5: *Specific heat capacity measurements as a function of temperature for the low-voltage Seacrete and the high-voltage Seacrete. The 1σ standard deviations are indicated in between brackets.*

Temperature [°C]	Specific heat capacity of the low-voltage Seacrete (1σ) [J/kg.K]	Specific heat capacity of the high-voltage Seacrete (1σ) [J/kg.K]
-60	690.6 (53.8)	-
-55	727.3 (49.0)	-
-50	736.4 (50.4)	-
-45	737.5 (46.2)	-
-40	748.8 (46.2)	-
-35	759.0 (46.2)	-
-30	769.9 (45.8)	-
-25	780.2 (46.0)	-
-20	789.0 (46.7)	-
-15	797.3 (46.9)	-
-10	806.5 (47.4)	-
-5	816.9 (47.5)	-
0	823.7 (47.5)	-
5	823.6 (47.8)	-
10	817.2 (48.3)	891.6 (39.9)

15	810.9 (48.5)	920.6 (46.9)
20	811.0 (48.5)	908.2 (27.3)
25	821.4 (48.4)	904.4 (41.2)
30	837.8 (48.5)	910.5 (33.8)
35	854.1 (49.2)	912.5 (33.7)
40	861.8 (52.3)	914.6 (39.9)
45	867.4 (57.5)	930.9 (31.9)
50	891.7 (58.8)	976.6 (33.0)
55	918.6 (59.8)	982.6 (43.6)
60	940.3 (59.7)	988.6 (22.6)
65	955.3 (59.0)	953.7 (26.3)
70	967.0 (58.2)	957.6 (27.0)
75	975.2 (58.2)	967.5 (31.0)
80	980.1 (58.1)	980.7 (17.7)
85	981.7 (58.3)	1004.9 (23.5)
90	980.9 (58.7)	1019.9 (17.8)

One can see in *Figure 6* that the Seacrete samples have a specific heat capacity that is very close to the calcium carbonate minerals Aragonite and Calcite [38][39]. The LV Seacrete has thus a specific heat capacity that is very close to that of its main mineral constituents. In the case of the HV Seacrete, although it is composed of half Brucite and half Aragonite, its specific heat capacity is also very close to that of the calcium carbonate minerals, and significantly lower than that of Brucite [40]. One can also notice that the Seacrete materials have a specific heat capacity at room temperature that is within the low range of typical concrete and natural stone materials of similar density. The latter is used for building construction and have a specific heat capacity commonly ranging from 800 to 1200 J/kg K [37]. Consequently, the Seacrete materials have a volumetric heat capacity that is very similar to concrete, natural stone and ceramic materials of equivalent density. In addition, the specific heat capacity of the Seacrete samples is very close to the standard value for concrete material (Eurocode 2 - EN 1992-1-2:2004 (E) [41]).

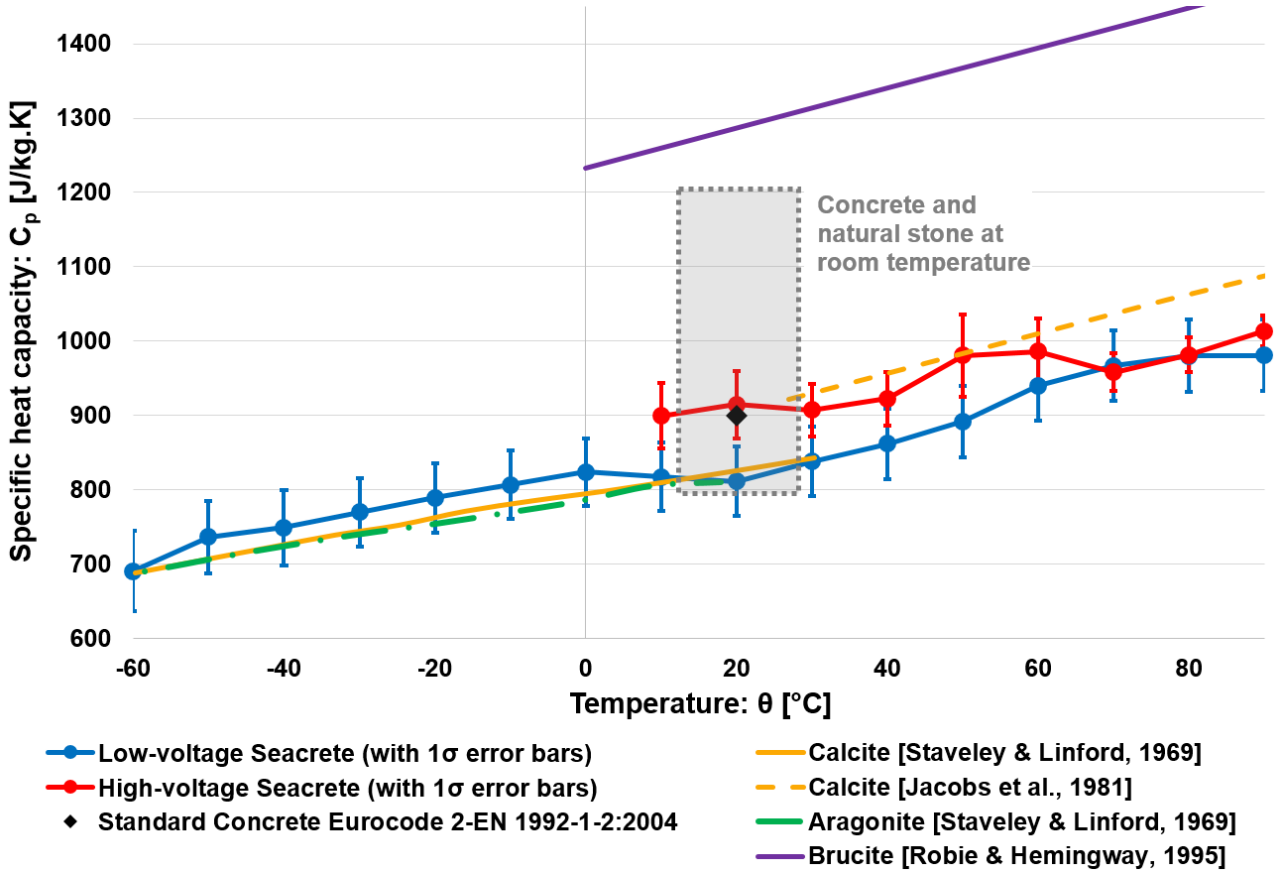

Figure 6: *Specific heat capacity comparison of the low-voltage Seacrete and the high-voltage Seacrete with different calcium carbonate minerals and Brucite mineral together with concrete and natural stone at room temperature [37][38][39][40][41].*

4.3.2. Thermal diffusivity measurements

One can see in *Figure 7* and in *Table 6* the thermal diffusivity measurements of the Seacrete samples within the temperature range 10°C to 60°C. It can be observed that, in that temperature range, the thermal diffusivity tends to decrease linearly with the increasing temperature. One can also notice that the thermal diffusivity of the HV Seacrete is significantly lower than that of the LV Seacrete. Because the HV Seacrete has a specific heat capacity that is similar to that of the LV Seacrete, and because the HV Seacrete has a bulk density that is only 29% lower than that of the LV Seacrete, it may be presumed that the lower thermal diffusivity of the HV Seacrete is linked to a lower thermal conductivity induced by its higher porosity compared to the LV Seacrete.

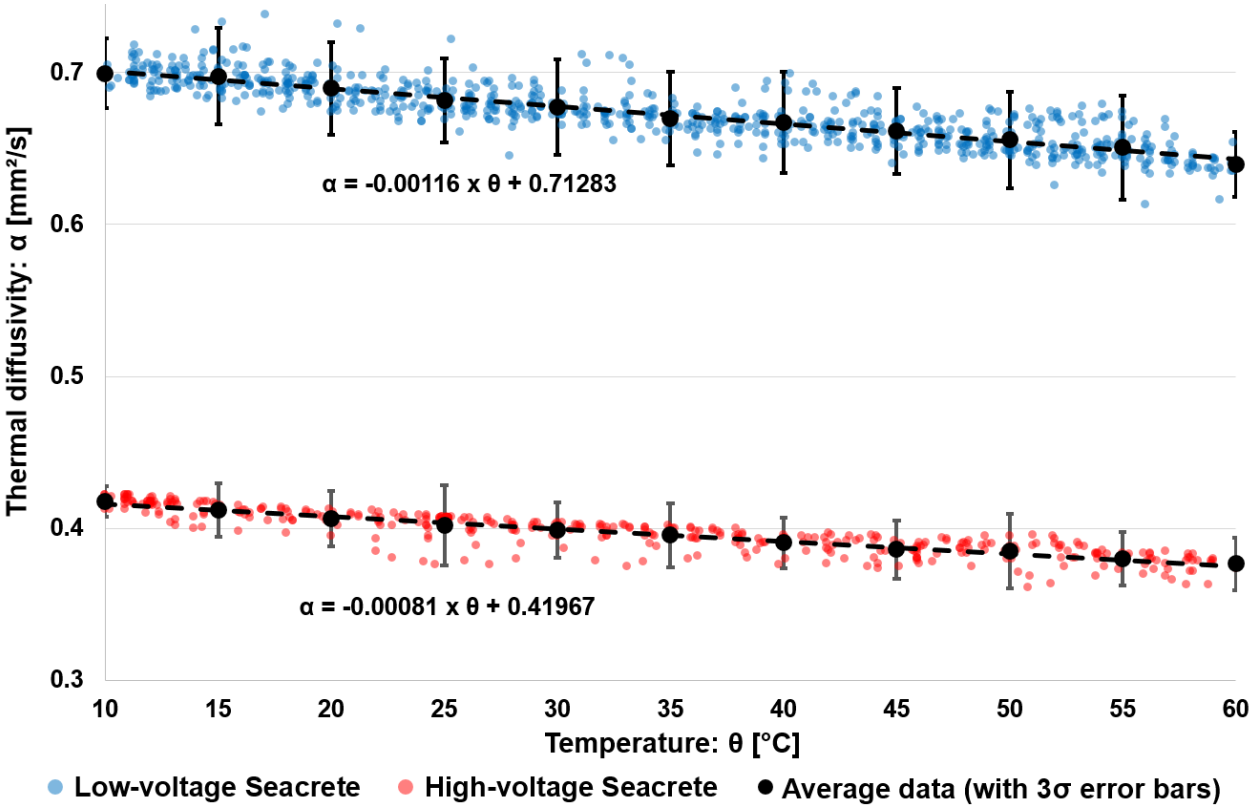

Figure 7: *Measurements of the thermal diffusivity of the low-voltage Seacrete and the high-voltage Seacrete as a function of temperature with linear fitting functions.*

Table 6: *Thermal diffusivity measurements as a function of temperature for the low-voltage Seacrete and high-voltage Seacrete. The 1σ standard deviations are indicated in between brackets.*

Temperature [°C]	Thermal diffusivity of the low-voltage Seacrete (1σ) [mm²/s]	Thermal diffusivity of the high-voltage Seacrete (1σ) [mm²/s]
10	0.6994 (0.0077)	0.4176 (0.0033)
15	0.6976 (0.0105)	0.4121 (0.0059)
20	0.6897 (0.0102)	0.4066 (0.0061)
25	0.6816 (0.0093)	0.4021 (0.0087)
30	0.6771 (0.0104)	0.3990 (0.0060)
35	0.6698 (0.0103)	0.3956 (0.0070)
40	0.6672 (0.0111)	0.3905 (0.0055)
45	0.6616 (0.0094)	0.3862 (0.0064)
50	0.6556 (0.0106)	0.3853 (0.0082)
55	0.6507 (0.0114)	0.3801 (0.0059)
60	0.6395 (0.0072)	0.3766 (0.0057)

One can see in *Figure 8* that the LV Seacrete has a thermal diffusivity that is very close to Aragonite [42]. It should be noted that the thermal diffusivity of the Aragonite has been derived from the thermal conductivity data of Aragonite in the nacre of shells since no other appropriate data has been found. One can also notice that the LV Seacrete has a

thermal diffusivity at room temperature that is within the low range of that of a typical concrete (Eurocode 2 - EN 1992-1-2:2004 (E) [41]). In addition, the LV Seacrete has a thermal diffusivity within the range of typical natural stone and concrete materials of similar density that are used for building construction and have a thermal diffusivity commonly ranging from 0.3 to 1.6 mm^2/s [37].

In the case of HV Seacrete, one can see that its thermal diffusivity is significantly lower than that of the LV Seacrete, the calcium carbonates, and the standard concrete. However, it lies within the low range of thermal diffusivity for typical natural stone and concrete materials of similar density.

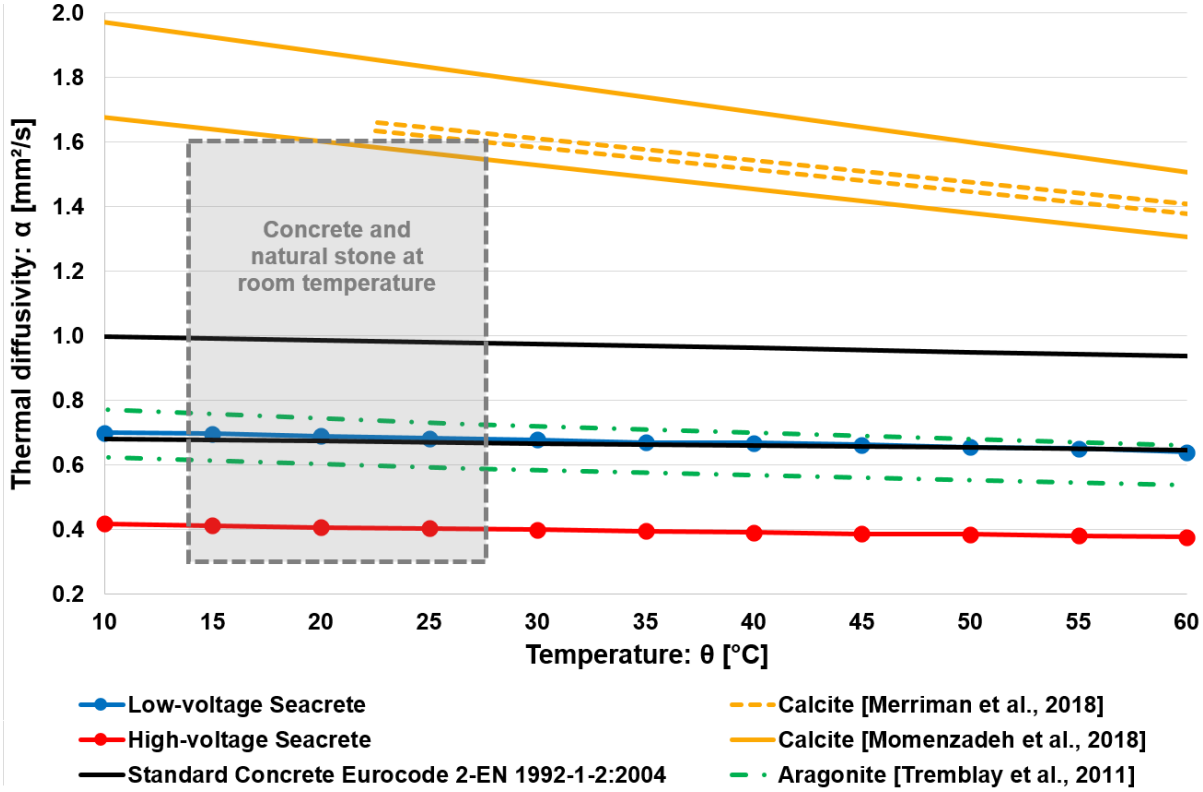

Figure 8: *Thermal diffusivity comparison of the low-voltage Seacrete and the high-voltage Seacrete with different calcium carbonate minerals together with concrete and natural stone at room temperature [37][41][42][43][44].*

4.3.3. Calculated thermal conductivity

From the measurement results of density, specific heat capacity and thermal diffusivity presented previously, the thermal conductivity of the Seacrete material is calculated. It should be noted that the density of the material is assumed to be independent of the temperature and equal to the measurement conducted at 20°C. One can see in *Figure 9* and in *Table 7* the calculated thermal conductivity of the Seacrete for temperatures ranging from 10°C to 60°C. One can observe that the thermal conductivity of the HV Seacrete is significantly lower than that of the LV Seacrete. As previously mentioned for the thermal diffusivity, the difference in thermal conductivity between the two Seacrete materials can be explained by the difference in porosity. The HV Seacrete has a higher porosity and thus more air-filled pores with low thermal conductivity, which results in an overall lower global thermal conductivity compared to the LV Seacrete.

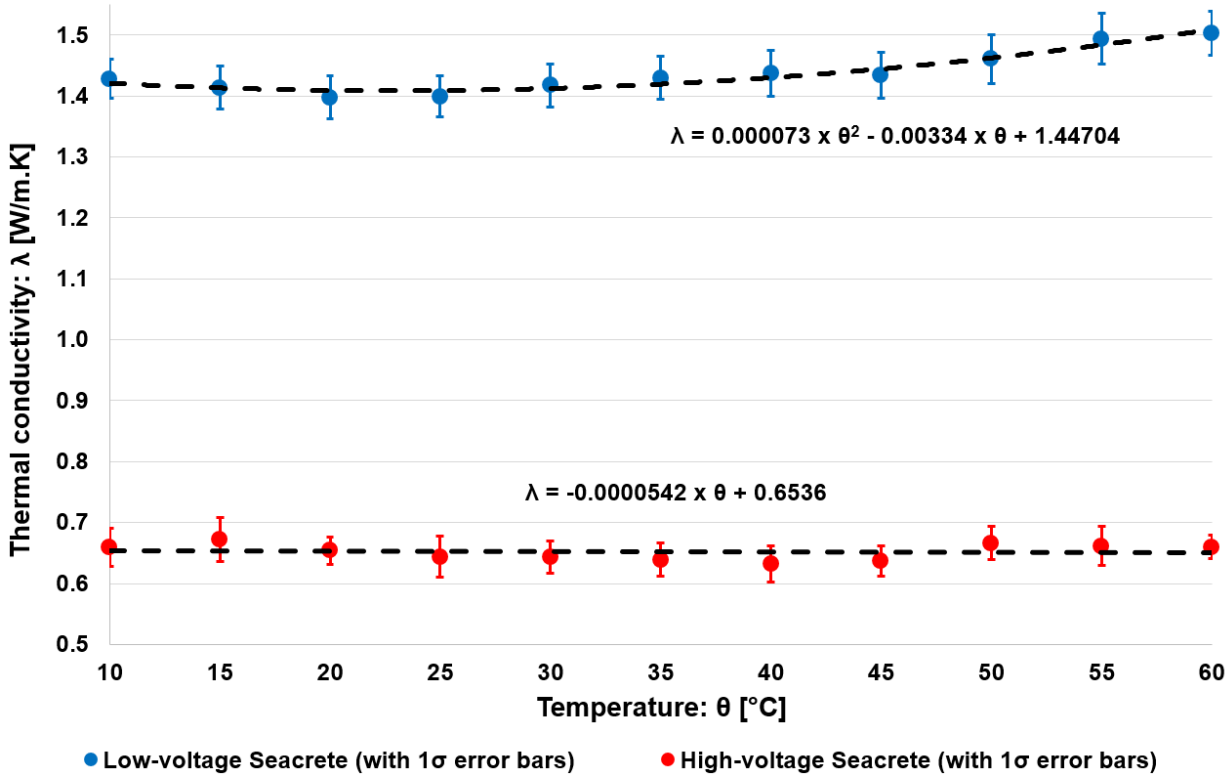

Figure 9: *Calculated thermal conductivity of the low-voltage Seacrete and the high-voltage Seacrete as a function of temperature with polynomial fitting functions.*

Table 7: *Calculated thermal conductivity as a function of temperature for the low-voltage Seacrete and high-voltage Seacrete. The 1σ standard deviations are indicated in between brackets.*

Temperature [°C]	Thermal conductivity of the low-voltage Seacrete (1σ) [W/m K]	Thermal conductivity of the high-voltage Seacrete (1σ) [W/m K]
10	1.428 (0.086)	0.659 (0.031)
15	1.414 (0.087)	0.672 (0.036)
20	1.398 (0.086)	0.654 (0.023)
25	1.399 (0.085)	0.644 (0.033)
30	1.418 (0.085)	0.643 (0.027)
35	1.430 (0.085)	0.639 (0.027)
40	1.437 (0.091)	0.633 (0.030)
45	1.434 (0.097)	0.637 (0.025)
50	1.461 (0.099)	0.666 (0.027)
55	1.494 (0.101)	0.661 (0.032)
60	1.503 (0.097)	0.659 (0.019)

Similarly to the thermal diffusivity results, one can see in *Figure 10* that the LV Seacrete has a thermal conductivity that is very close to Aragonite [42]. One can also notice that the LV Seacrete has a thermal conductivity at room temperature that is within the low range of the thermal conductivity for a standard concrete (Eurocode 2 - EN 1992-1-2:2004 (E) [41]). In addition, the Seacrete material has a thermal conductivity within the range of typical natural stone

and concrete materials of similar density that are used for building construction and have a thermal conductivity commonly ranging from 0.5 to 3.5 W/m K [37].

In the case of HV Seacrete, one can see that its thermal conductivity is significantly lower than that of the LV Seacrete, the calcium carbonates, and the standard concrete. However, it lies within the low range of thermal conductivity for typical natural stone and concrete materials of similar density.

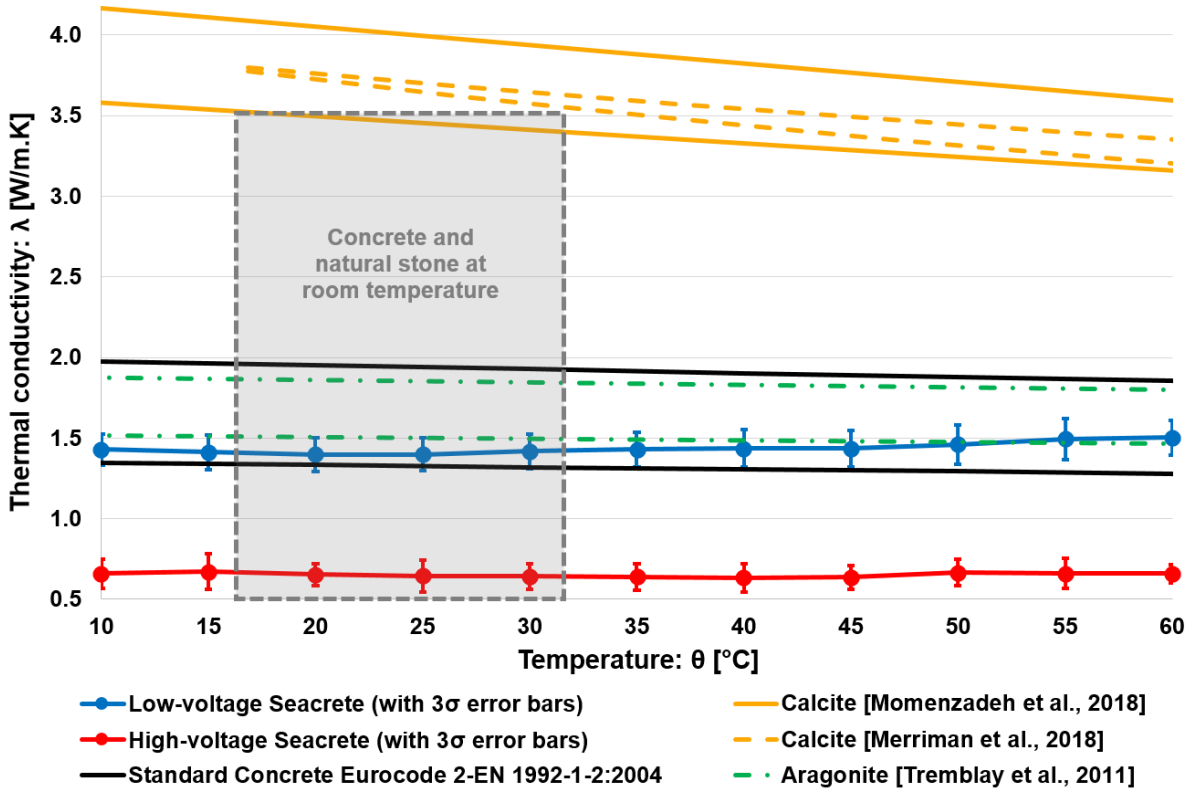

Figure 10: *Thermal conductivity comparison of the low-voltage Seacrete and the high-voltage Seacrete with different calcium carbonate minerals together with concrete and natural stone at room temperature [37][41][42][43][44].*

4.4. Moisture sorption-desorption capacity measurements

Figure 11 shows the isotherms of the three investigated materials and their respective GAB fitting models (described by equation (2) with the GAB model parameters given in *Table 8*). The amount of water vapour is given on dry mass basis for the relative humidity in the VSA chamber ranging from 3% to 93%. One can clearly observe that none of the materials exhibit significant temporal moisture dynamics (changes in the isotherm shape and/or magnitude) from one cycle to the next one. It can thus be considered that the response surface of those materials may be defined by a single isotherm. The LV Seacrete and concrete present relatively similar isotherm shape and capacity to exchange and store water vapour. This is expected since the materials have similar densities and pore size distributions. The HV Seacrete material has an isotherm of similar shape with, however, a larger magnitude in the higher relative humidity range (~60 – 93% RH).

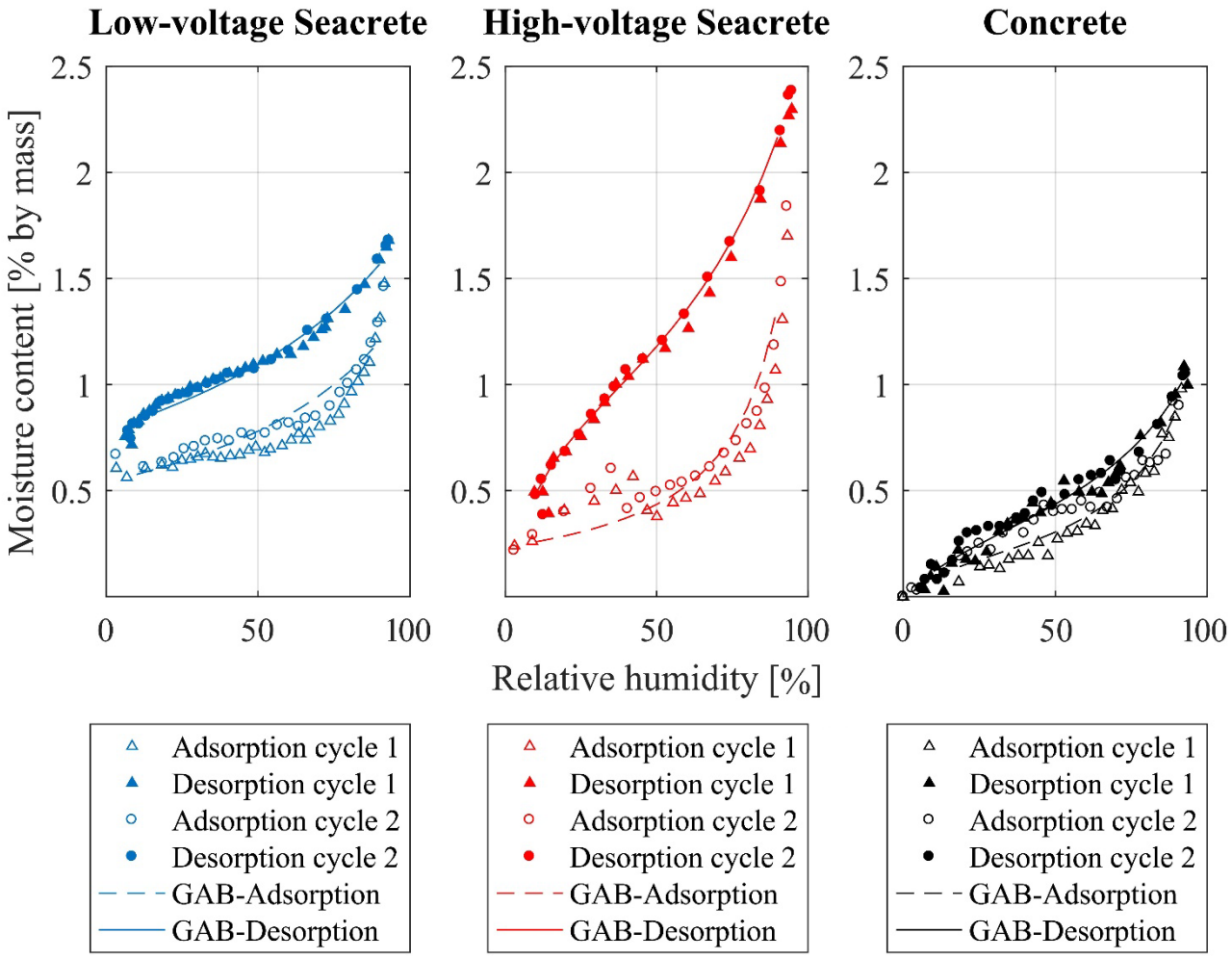

Figure 11: *Isotherms from VSA measurements and GAB fitting models for low-voltage Seacrete (left), high-voltage Seacrete (center), and concrete (right).*

The resulting hysteresis index at three specific relative humidity points (25%, 50% and 75%) can be found in *Table 8*. The HV Seacrete presents a lower density and a higher porosity, inducing a larger hysteresis at all three relative humidity points. This indicates that HV Seacrete is expected to have the largest and/or most connected open pores and thus the highest potential for moisture buffering. This corroborates well with the aforementioned mechanical resistance results.

One can also find in *Table 8* the GAB coefficients that are necessary to approximate the moisture content of the material based on the relative humidity. Despite that the GAB model is mainly applied for soil and food science, recent research has shown that it is applicable to building materials as well [45]. R^2, the coefficient of determination of the GAB model compared to the moisture content measurement data is also included in the table. It should be noted that all the parameters presented in *Table 8* are calculated based on the isotherm of on both isotherm cycles of the VSA measurements. Assuming that there is a monolayer of water formed on the material surfaces at 21% RH, the water active surface area of the each material is calculated from the moisture content measurements at 21% RH (see *Table 8*). The results suggest that LV Seacrete possesses the largest water active surface areas compared to HV Seacrete and concrete.

Table 8: *Moisture properties obtained by experimentally derived isotherms of the Seacrete materials compared to tested concrete.*

GAB model		Low-voltage Seacrete	High-voltage Seacrete	Concrete
Absorption	C [-]	10403	10980	7.336

	K [-]	0.611	0.92	0.863
	W_m [% by mass]	0.542	0.235	0.204
	R^2 [-]	0.88	0.935	0.94
Desorption	C [-]	1067	14.42	5.577
	K [-]	0.546	0.675	0.722
	W_m [% by mass]	0.798	0.888	0.368
	R^2 [-]	0.99	0.99	0.96
Hysteresis [%]	@25% RH	0.295	0.325	0.285
	@50% RH	0.362	0.730	0.485
	@75% RH	0.479	0.985	0.425
Surface area [m^2/gr]		23.6	17.4	6.1

5. Summary and conclusions

Seacrete appears to be an interesting alternative to traditional cementitious materials for construction applications that do not require high mechanical resistance. It has therefore attracted some attention over the last years. However, previous publications about Seacrete only reported some of its mechanical characteristics without any focus on its thermal and hygroscopic properties. This article is thus the first publication to provide an experimental analysis of the thermal and moisture properties of the Seacrete material. The dry bulk density, the compression strength, the puncture resistance, the specific heat capacity, the thermal diffusivity, the thermal conductivity, and the water vapour sorption isotherms of two types of Seacrete (low-voltage Seacrete and high-voltage Seacrete) have been measured at near room-temperature. This information is crucial for the application of Seacrete as a construction material in the fields of building structure, building hygro-thermodynamics and indoor environment. These experimental results have been compared with the material properties of concrete (either from experimental tests conducted during this study, or found in the scientific literature). One can find in *Table 9* a summary of the mechanical, thermal and moisture properties of the tested Seacrete materials and concrete.

The main conclusion of this experimental investigation is that Seacrete materials have mechanical, thermal and hygroscopic properties that are comparable to that of concrete materials. More specifically, the low-voltage Seacrete presents hygrothermal properties that are very close to that of standard concrete and a mechanical resistance that is very similar to that of a mortar of compressive strength class C20/25. Concerning the high-voltage Seacrete, because it has a larger porosity than the low-voltage Seacrete, its density, mechanical resistance, thermal conductivity and thermal diffusivity are significantly lower than that of concrete. However, those material properties are within the low range of natural stones and concrete materials with a similar density that are commonly used for building construction. In addition, the high-voltage Seacrete presents a more open-pore structure which confers it a larger “breathability” and a greater moisture buffering capacity.

The current experimental analysis provides clear evidence that Seacrete materials can perform similarly to concrete for some structural and thermodynamic applications in constructions. These experimental results support the previous publications claiming that Seacrete has the necessary mechanical resistance to substitute concrete in certain building’s infrastructures such as low-rise indoor construction elements. In addition, the current investigation points out that Seacrete has similar thermal properties as concrete, meaning that it can offer the same effective thermal inertia. The latter is of prime importance to ensure the temperature stability of the indoor environment, decrease the risks of overheating, reduce cooling peaks, and offer thermal storage capacity for energy flexibility strategies and demand-side management. Similarly, the higher moisture buffering capacity of the high-voltage Seacrete is an asset to stabilize the relative humidity of the indoor space and thus improve the indoor air quality and the occupants’ thermal comfort.

This study also confirms the trade-off between the Seacrete material growth rate and its mechanical resistance. Faster production of Seacrete with high-voltage electrodeposition generates a material with a higher content of softer Brucite mineral, and with higher porosity, and thus a lower mechanical strength.

Table 9: *Summary of the mechanical, thermal and moisture properties (standard room-conditions of temperature, humidity and pressure) of the Seacrete materials compared to concrete.*

Material properties		**Low-voltage Seacrete**	**High-voltage Seacrete**	**Concrete**
Density [kg/m^3]		2499.2	1771.1	1800 – 2400 [a]
Compression strength [MPa]		Not measured	16.8 [b]	24.2 [b]
Puncture resistance [kN]		3.9 [c]	1.4 [c]	3.4 [c]
Specific heat capacity [J/kg.K]		811 [d]	908.2 [d]	900 [e]
Thermal diffusivity [mm^2/s]		0.6897 [f]	0.4066 [f]	0.99 – 0.67 [e]
Thermal conductivity [W/m.K]		1.398 [g]	0.654 [g]	1.95 – 1.33 [e]
Moisture absorption [h] (GAB model)	C [-]	10403	10980	7.336
	K [-]	0.611	0.92	0.866
	W_m [% by mass]	0.542	0.235	0.204
	R^2 [-]	0.88	0.935	0.94
Moisture desorption [h] (GAB model)	C [-]	1067	14.42	5.577
	K [-]	0.546	0.675	0.722
	W_m [% by mass]	0.798	0.888	0.366
	R^2 [-]	0.99	0.99	0.96
Moisture hysteresis [%] [h]	@25% RH	0.295	0.325	0.285
	@50% RH	0.362	0.730	0.485
	@75% RH	0.479	0.985	0.425
Surface area [m^2/gr] [h]		23.6	17.4	6.1

[a] Refer to Johra 2019 [37].

[b] Down scaled compression test on 1 x 1 x 1 cm cubical sample: refer to *Table 4*.

[c] Non-standard penetration test on 1 x 1 x 1 cm or 1 x 1 x 0.4 cm cubical sample: refer to *Table 4*.

[d] At a temperature of 20 °C: refer to *Table 5*.

[e] Refer to Eurocode 2 - EN 1992-1-2:2004 (E) [41].

[f] At a temperature of 20 °C: refer to *Table 6*.

[g] At a temperature of 20 °C: refer to *Table 7*.

[h] GAB model parameter: refer to *Table 8*.

6. Suggestions for future work

Despite the enthusiasm of certain architects for self-growing structures and sea-grown construction materials, and the use of Seacrete for the restoration of coral reefs and marine ecosystems, this technology is relatively young and requires further scientific investigations on its applicability in the building and construction sectors. The authors would like to suggest some topics of interest for future work on the Seacrete building material:

- Further experimental tests and material characterizations on larger Seacrete samples and full-scale construction elements with aggregates and steel frames covered and bound by the electrodeposited Seacrete.
- Comparison of the Seacrete materials with different types and classes of cementitious products: cement paste, mortar, concrete, reinforced concrete elements.
- Study of the thermal dilatation, hygroscopic swelling and shrinkage, chemical stability and durability of Seacrete materials and Seacrete full-scale construction elements.

- Investigations of the different production parameters affecting the growth rate of the Seacrete and its chemical composition, porosity, mechanical, thermal and hygroscopic properties: seawater composition and temperature, cathode properties, applied voltage, etc.
- Study of the local and global impacts of Seacrete production on the seawater acidification and the CO_2 balance.
- Economic cost analysis of Seacrete material used for building construction.
- CO_2 footprint calculation and Life Cycle Assessment (LCA) of the Seacrete building material.
- Testing other important material characteristics of the Seacrete for building and indoor space utilization such as acoustic and lighting properties.

Acknowledgements

The authors would like to express their gratitude to Leonid Gurevich for his help in performing SEM imaging.

Conflict of interest

The authors declare that they do not have competing financial interest, personal relationship or any kind of known conflict of interest that could have influenced the work reported in this article.

References

[1] 2018 Global Status Report: towards a zero-emission, efficient and resilient buildings and construction sector, International Energy Agency and the United Nations Environment Programme, 2018, https://wedocs.unep.org/bitstream/handle/20.500.11822/27140/Global_Status_2018.pdf.
[2] GNR Project Reporting CO2 - WBCSD Cement Sustainability Initiative - Getting the Numbers Right Project - Emissions Report 2017, World Business Council for Sustainable Development, 2017.
[3] The cement sustainability initiative, our agenda for action, World Business Council for Sustainable Development, July 2002.
[4] R.M. Andrew, CO2 emissions from cement production, 1928 – 2017, Earth System Science Data 10 (2018) 2213–2239.
[5] A. Torres, J. Brandt, K. Lear, J. Liu, A looming tragedy of the sand commons, Science 357 (2017) 970–971.
[6] W.H. Hilbertz, Mineral accretion of large surface structures, building components and elements, US Patent No. 4246075 (A), 1981.
[7] L. Margheritini, P. Møldrup, R.L. Jensen, K.M. Frandsen, Y.I. Antonov, K. Kawamoto, L.W. de Jonge, R. Vaccarella, T.L. Bjørgård, M.E. Simonsen, Coral relief materials: Comparative physical-chemical properties of biorock, high-voltage sea deposit, and coral reef samples, Scientific Reports (under review).
[8] W.H. Hilbertz, Electrodeposition of Minerals in Sea Water: Experiments and Applications, IEEE J Ocean Eng 4 (1979) 94–113.
[9] T.J. Goreau, Marine Electrolysis for Building Materials and Environmental Restoration. In: J. Kleperis, V. Linkov, editors, Electrolysis, 2012.
[10] T.J. Goreau, Electrical Stimulation Greatly Increases Settlement, Growth, Survival, and Stress Resistance of Marine Organisms, Nat Resour 5 (2014) 527–537.
[11] M. Kummu, H. De Moel, G. Salvucci, D. Viviroli, P.J. Ward, O. Varis, Over the hills and further away from coast: Global geospatial patterns of human and environment over the 20th-21st centuries. Environ Res Lett. 11 (3) (2016).
[12] L. Margheritini, G. Colaleo, P. Contestabile, T.L. Bjørgård, M.E. Simonsen, C. Lanfredi, A. Dell'Anno, D. Vicinanza, Development of an Eco-Sustainable Solution for the Second Life of Decommissioned Oil and Gas Platforms: The Mineral Accretion Technology, Sustainability 12 (2020) 3742.
[13] J.C. Calero, M.C. Llorca, P.G. Terradillos, Influence of different ways of chloride contamination on the efficiency of cathodic protection applied on structural reinforced concrete elements, Journal of Electroanalytical Chemistry 793 (2017) 8-17.
[14] G. Terlouw G (2012). Coral reef rehabilitation on Koh Tao, Thailand: Assessing the success of a Biorock artificial reef, New Heaven Reef Conservation Program & Vrije Universiteit Amsterdam, 2012.
[15] C. Barchiche, C. Deslouis, O. Gil, P. Refait, B. Tribollet, Characterisation of calcareous deposits by electrochemical methods:role of sulphates, calcium concentration and temperature, Electrochimica Acta 49 (2004) 2833–2839.
[16] EN 206:2013 + A1:2016(E), Concrete - Specification, performance, production and conformity, British Standards Institution (BSI), 2016.
[17] The White Guide, Aalborg Portland White A/S, 2006, https://www.aalborgwhite.com/media/pdf_files/info_the_white_guide.pdf.
[18] Density measurement, Mettler Toledo, https://www.mt.com/ch/en/home/applications/Laboratory_weighing/density-measurement.html.
[19] BS EN 196-1:2016, Methods of testing cement. Determination of strength, British Standards Institution (BSI), 2016.
[20] MTS model 810, MTS Systems Corporation, https://www.upc.edu/sct/documents_equipament/d_77_id-412.pdf.
[21] A Summary of Error Propagation, Harvard University, 2007, http://ipl.physics.harvard.edu/wp-uploads/2013/03/PS3_Error_Propagation_sp13.pdf.
[22] E.S. Watson, M.J. O'Neill, Differential microcalorimeter, US Patent No. 3263484A, 1962.
[23] Thermal Analysis Brochure, TA Instruments, Inc., 2012, https://www.tainstruments.com/pdf/brochure/2012%20DSC%20Brochure%20r1.pdf.
[24] Hicham Johra, Description of the laser flash analysis method for thermal diffusivity measurement with the LFA 447, DCE Lecture Notes No. 73, Department of Civil Engineering, Aalborg University, 2019, https://vbn.aau.dk/ws/portalfiles/portal/312969074/Description_of_the_Laser_Flash_Analysis_Method_for_Thermal_Diffusivity_Measurement_with_the_LFA_447.pdf.
[25] Operating Instructions Nano-Flash-Apparatus LFA 447, Netzsch Gerätebau GmbH, 2001.
[26] Vapor Sorption Analyzer from AquaLab, https://www.metergroup.com/food/products/vsa/.

[27] EN ISO 12571:2013, Hygrothermal performance of building materials and products - Determination of hygroscopic properties, International Organization for Standardization, 2013.
[28] Y.A. Antonov, K.M. Frandsen, P. Møldrup, E. Arthur, L.W. de Jonge, M. Pomianowski, R.L. Jensen, Linking Comparing Three Methods for Quantifying Water Vapor Sorption Dynamics in Bio-based Building Materials, Energy and Buildings (under review).
[29] R.D.P. Andrade, L.M. Roberto, C.E.C. Pérez, Models of sorption isotherms for food: Uses and limitations - Modelos de isotermas de sorcion para alimentos: Usos y limitaciones, Vitae. 18 (2011) 325–334.
[30] E. Arthur, M. Tuller, P. Møldrup, M.H. Greve, M. Knadel, L.W. De Jonge, Applicability of the Guggenheim – Anderson – Boer water vapour sorption model for estimation of soil specific surface area, European Journal of Soil Science (2018) 245–255.
[31] J.P. Quirk, R.S. Murray, Appraisal of the Ethylene Glycol Monoethyl Ether Method for Measuring Hydratable Surface Area of Clays and Soils. Soil Science Society of America Journal 63 (1999) 839–849.
[32] B. Lafuente, R.T. Downs, H. Yang, N. Stone, The power of databases: the RRUFF project, In: Highlights in Mineralogical Crystallography, T. Armbruster and R.M. Danisi, editors. Berlin, Germany, W. De Gruyter, 2015.
[33] Aragonite, RRUFF Project, http://rruff.info/doclib/hom/aragonite.pdf.
[34] Vaterite, RRUFF Project, http://rruff.info/doclib/hom/vaterite.pdf.
[35] Calcite, RRUFF Project, http://rruff.info/doclib/hom/calcite.pdf.
[36] Brucite, The Mineral Website, http://webmineral.com/data/Brucite.shtml#.Xg9nu_lKibg.
[37] Hicham Johra, Thermal properties of common building materials, DCE Technical Reports No. 216, Department of Civil Engineering, Aalborg University, 2019, https://vbn.aau.dk/ws/portalfiles/portal/294603722/Thermal_properties_of_common_building_materials.pdf.
[38] L.A.K. Staveley, R.G. Linford, The heat capacity and entropy of calcite and aragonite, and their interpretation, The Journal of Chemical Thermodynamics 1 (1969) 1–11.
[39] G.K. Jacobs, D.M. Kerrick, K.M. Krupka, The high-temperature heat capacity of natural calcite (CaCO3), Physics and Chemistry of Minerals 7 (2) (1981) 55–59.
[40] R.A. Robie, B.S. Hemingway, Thermodynamic Properties of Minerals and Related Substances at 298.15 K and 1 Bar (10^5 Pascals) Pressure and at Higher Temperatures, U.S. Geological Survey Bulleting (1995) 2131.
[41] EN 1992-1-2:2004 (E), Eurocode 2: Design of concrete structures - Part 1-2: General rules - Structural fire design, European Committee for Standardization (CEN), 2004.
[42] L.P. Tremblay, M.B. Johnson, U. Werner-Zwanziger, M.A. White, Relationship between thermal conductivity and structure of nacre from Haliotis fulgens, Journal of Materials Research 26 (2011) 1216–1224.
[43] J.D. Merriman, A.M. Hofmeister, D.J. Roy, A.G. Whittington, Temperature-dependent thermal transport properties of carbonate minerals and rocks, Geosphere 14 (4) (2018) 1961–1987.
[44] L. Momenzadeh, B. Moghtaderi, O. Buzzi, X. Liu, S.W. Sloan, G.E. Murch, The thermal conductivity decomposition of calcite calculated by molecular dynamics simulation, Computational Materials Science 141 (2018) 170–179.
[45] K.M. Frandsen, Y.I. Antonov, P. Møldrup, R.L. Jensen, Water vapor sorption dynamics in different compressions of eelgrass insulation, E3S Web Conf., 172 (2020) 17005, DOI: https://doi.org/10.1051/e3sconf/202017217005.